Angel D. A. Acosta-Solórzano[1]
Oscar Guerrero-Farfán[1]
César Ramírez-Márquez[1]
Fernando I. Gómez-Castro[1]
Juan Gabriel Segovia-Hernández[1]
Salvador Hernández[1]
Claudia Gutiérrez-Antonio[2]
Abel Briones-Ramírez[3]

[1]Universidad de Guanajuato, Campus Guanajuato, División de Ciencias Naturales y Exactas, Departamento de Ingeniería Química, Guanajuato, México.

[2]Facultad de Química, Universidad Autónoma de Querétaro, Las Campanas, Querétaro, México.

[3]Exxerpro Solutions, Querétaro, México.

Supporting Information available online

Controllability Analysis of Distillation Sequences for the Separation of Bio-Jet Fuel and Green Diesel Fractions

The aviation sector is nowadays looking for a biofuel to partially substitute the fossil fuel used for flights, i.e., jet fuel. Among the proposed processes for the production of the renewable jet fuel, the hydrotreating process has, to date, the best performance. At the final stage of the hydrotreating process, a distillation train is required to obtain hydrocarbon fractions useful as fuels. Conventional or thermally coupled distillation sequences can be used in this step, and it can be expected that thermally coupled sequences require less energy to perform the separation. Nevertheless, in the selection of the best sequence for a given separation, it is important to analyze its control properties. A controllability analysis was performed here for different distillation sequences used to obtain biofuels from a hydrocarbon renewable mixture, in order to detect the best sequence in terms of control properties.

Keywords: Bio-jet fuel, Controllability, Distillation sequences, Thermal coupling

Received: February 17, 2016; *revised:* April 18, 2016; *accepted:* September 9, 2016

DOI: 10.1002/ceat.201600095

1 Introduction

Interest in the production of biofuels has increased in the last decades, due to concerns regarding the actual availability of petroleum and the environmental impact associated with the continuous use of fossil fuels. In the particular case of transport fuels, the aviation sector contributes with about 2 % of the total annual anthropogenic emissions of carbon dioxide [1]. Furthermore, it has been predicted that the global emissions due to international aviation will grow by about 700 % by 2020, compared with those of 2005 [2]. The most promising strategy to reduce the environmental impact of the air transport industry is to use biofuels for the flights. The liquid biofuel used for such applications is known as bio-jet fuel, and it is usually composed of a mixture of hydrocarbons known as synthetic paraffinic kerosenes (SPK). The physical and chemical properties of bio-jet fuel must be very similar to those of fossil jet fuel, in order to avoid operational problems in the planes. Nevertheless, SPK contain no aromatics; thus, they must be used in mixtures of up to 50 % of fossil jet fuel [3].

One of the most studied methods for the production of SPK is the hydrotreating process, patented by UOP Honeywell [4]. The process consists basically of the conversion of the triglycerides from vegetable oils into long-chain hydrocarbons by hydrotreating reactions, followed by simultaneous hydrocracking and isomerization of those hydrocarbons to obtain a portion of ramified molecules. Then, the fractions are refined in distillation columns to obtain the desired products, which are mainly light hydrocarbons, bio-jet fuel, and green diesel. A representation of the whole process is shown in Fig. 1. In a recent work [5], alternatives have been proposed for the separation of those three fractions. Since three products are obtained, there are two conventional ways to separate the mixture: a direct distillation sequence and an indirect distillation sequence. Gutiérrez-Antonio et al. [5] optimized two conventional separation sequences and four thermally coupled sequences, and found that the thermally coupled direct sequence (TCDS) shows the lowest energy requirements for the production of bio-jet fuel and green diesel. Nevertheless, in order to establish the best sequence for a given separation, it is also important to have information about their dynamic performance.

There are two traditional approaches to evaluate the dynamic properties of a system: open-loop and closed-loop analysis. Open-loop analysis involves the study of the natural dynamics

Correspondence: Fernando Israel Gomez-Castro (fgomez@ugto.mx, iq_fergo@hotmail.com), Universidad de Guanajuato, Campus Guanajuato, División de Ciencias Naturales y Exactas, Departamento de Ingeniería Química, Noria Alta S/N Col. Noria Alta, Guanajuato, México 36050.

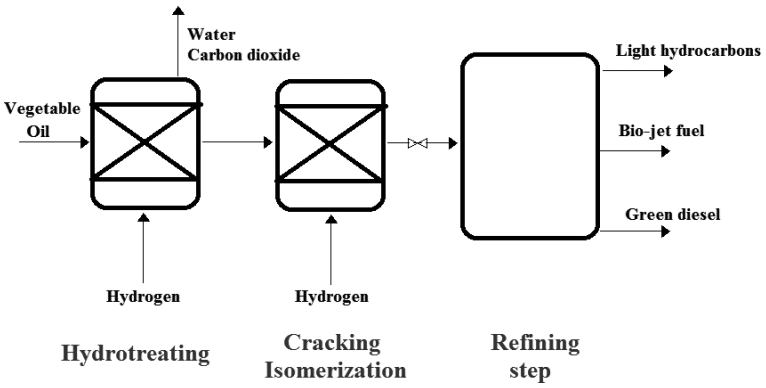

Figure 1. Simplified representation of the hydrotreating process.

of a process. In other words, the natural response of a given system to a perturbation is studied, with no controllers involved. Such an analysis has previously been used as a preliminary strategy to compare different configurations in terms of their dynamic properties. Hernández and Jiménez [6] found that the thermally coupled sequences with side columns have better open-loop control properties than the Petlyuk column, but the last sequence has lower energy requirements. Also, Jiménez et al. [7] reported an analysis of the control properties of distillation sequences with side stream and thermally coupled distillation sequences. They reported that complex configurations not necessarily have bad control properties in comparison with conventional sequences. Gómez-Castro et al. [8, 9] studied the open-loop properties of columns with single and double dividing-wall columns (DWC), finding that, for a hydrocarbon mixture with a low content of the middle-boiling component, the existence of two dividing walls may enhance the open-loop control properties. Hwang et al. [10] presented an open-loop dynamic study on a DWC, comparing the effects of the cross-pairing for the control loops on the side and bottom products.

On the other hand, closed-loop analysis involved the study of the response of a system subjected to disturbances when a controller is linked to a pairing in the input/output variables; the best control strategy is chosen, usually by the selection of the most reliable set of values for the tuning parameters of the controller. There are many works dealing with the closed-loop control of thermally coupled distillation systems. Segovia-Hernández et al. [11] presented a closed-loop analysis for thermally coupled distillation sequences, including the Petlyuk column, reporting better configurations for proportional-integral (PI) controllers in terms of the minimization of the integral of the squared error (ISE) and integral of the absolute error (IAE) criteria. Zhu et al. [12] compared three different closed-loop control strategies for thermally coupled distillation columns: a conventional proportional-integral-derivative (PID) control, a predictive PID control, and a robust PID control. According to their results, all the proposed strategies allowed good responses to disturbances, but the predictive PID was the best among the three cases. In another work [13], the use of a PI controller with disturbance estimation was proposed for the control of a Petlyuk column, finding better closed-loop responses when compared with those of a PI controller. Segovia-Hernández et al. [14] performed a closed-loop analysis of thermally coupled distillation sequences under various operational conditions. They concluded that the designs with the lowest energy requirements for a given sequence have worse control properties than the non-optimal designs. Strategies have also been proposed to control DWC by measuring impurities in the product streams instead of the purities of the desired products [15]. Recently, advanced control strategies for the control of thermally coupled systems have been proposed, such as model predictive control [16–18] and fuzzy control [19], among others. Also recently, Ramírez-Corona et al. [20] presented a control analysis of thermally coupled distillation columns, considering not only the isolated equipment but the interactions with whole processes.

From the review of the literature, it is clear that the use of closed- and open-loop analysis for controllability studies has been widely used in a great variety of processes. However, few controllability studies have been performed for the production process of biofuels. There are few works for biodiesel focusing on the closed-loop analysis in a reactive absorption process [21], reactive and extractive thermally coupled distillation sequences [22], reactive DWC [23], and a production process using a sugar catalyst [24]; also, some works for bioethanol have been reported, like closed-loop analysis in an extractive distillation process using glycerol as entrainer [25] or different configurations based on conventional sequences for the purification of bioethanol [26]. However, for the hydrotreating process for the production of bio-jet fuel, no formal controllability analysis can be found. Therefore, in this work, open-loop and closed-loop analyses are performed for conventional and thermally coupled distillation sequences designed to obtain three products useful as renewable fuels: light gases, bio-jet fuel, and green diesel. A comparison of the dynamic properties for all the systems will indicate which sequence is the best in terms of controllability, and will give some insights on the impact of the location, in the Pareto front, of a given solution on their control properties for a mixture with a high number of components. The results show interesting relations between energy consumption and control properties of the systems under analysis.

2 Case of Study

The mixture to be separated is the effluent of the isomerization/cracking reactor of the hydrotreating process, as reported by Gutiérrez-Antonio et al. [5]. A total molar flow rate of 0.51 kmol h^{-1} is fed into the distillation train, the composition of which is shown in Tab. 1. The stream was treated to enter the refining step at 1.34 atm, as saturated liquid. It is important to notice that only normal hydrocarbons appear in the feed stream. Since this stream comes from an isomerization reactor, it contains also isomers. Nevertheless, due to the high quantity of isomers existing for long hydrocarbon chains, the normal molecule was taken as representative of all the possible isomers of each component.

Since the goal of the separation is to obtain three products, two conventional configurations can be used: a direct conven-

Table 1. Molar composition of the feed stream.

Component	Symbol	Composition [mol %]
Light hydrocarbons		
Propane	C3	9.04
n-Butane	*n*-C4	6.86
n-Pentane	*n*-C5	5.53
n-Hexane	*n*-C6	4.63
n-Heptane	*n*-C7	3.98
Bio-jet fuel		
n-Octane	*n*-C8	5.32
n-Nonane	*n*-C9	4.74
n-Decane	*n*-C10	4.27
n-Undecane	*n*-C11	3.89
n-Dodecane	*n*-C12	3.57
n-Tridecane	*n*-C13	3.29
n-Tetradecane	*n*-C14	3.06
n-Pentadecane	*n*-C15	0.26
n-Hexadecane	*n*-C16	0.26
Green diesel		
n-Heptadecane	*n*-C17	20.63
n-Octadecane	*n*-C18	20.67

tional distillation sequence (CDS) (Fig. 2 a) and an indirect conventional distillation sequence (CIS) (Fig. 2 b). Three thermally coupled distillation sequences were also analyzed. Two of them were directly obtained from the conventional sequences: the thermally coupled direct sequence (TCDS; Fig. 2 c) and the thermally coupled indirect sequence (TCIS; Fig. 2 d). The fourth analyzed system is the Petlyuk column (Fig. 2 e), whose physical application is the DWC.

The designs of the analyzed sequences are obtained from the work of Gutiérrez-Antonio et al. [5], where a multiobjective genetic algorithm with constraints is used to optimize all the structures. As a consequence of the two objectives, not a single design was obtained but a set of optimal designs, known as Pareto front. Thus, to perform the control analysis, different points from the Pareto front were selected. The selected designs, together with their respective total heat duty, are shown in Tab. S1. Two points were selected from a low-energy region, two from a high-energy region, and two intermediate points. It is worth mentioning that, for the DWC, only four points were selected. This is because the Pareto front showed only few feasible designs for such system.

3 Methodology

3.1 Open-Loop Analysis

In order to estimate the open-loop dynamic properties of the sequences under study, the singular value decomposition (SVD) technique was used. Through SVD analysis, it is possible to obtain information on the controllability of the systems. In a first stage, the steady-state simulations of the distillation sequences are exported to Aspen Dynamics as flow-driven simulations. In the dynamic environment, step changes are imposed on the manipulated variables, by 5 % over their nominal value. The responses of the measured variables are registered until a new steady state is achieved. The manipulated and measured variables are shown in Tab. S2, where C1 and C2 refer to the column tag, as shown in Fig. 2. It is important to notice that, since the products obtained are mixtures of various hydrocarbons, one of the purities of the components on the cut should be selected as measured variable. For the open-loop analysis, the purities of the key components were chosen as reference. This is the reason for the existence of more than one possibility of measured variables in Tab. S2. All the purities reported in Tab. S2 are molar purities.

Dynamic responses are adjusted to transfer functions and ordered in a transfer function matrix. Then, by using a MATLAB routine, SVD is applied to each matrix of transfer functions. SVD is a mathematic technique that decomposes a matrix $\mathbf{G}$ into three matrixes $\mathbf{V\Sigma W^H}$. $\mathbf{V}$ is a matrix of left singular vectors, $\mathbf{W^H}$ is a matrix of right singular vectors, and Σ is the matrix of singular values.[1)] In dynamic studies, the elements on the diagonal of Σ (known as singular values) are of particular interest. The smallest of the singular values is known as minimum singular value ($\sigma*$), and it is a measurement of the potential difficulties observed when a closed-loop feedback control is implemented. Thus, high minimum singular values are desired for a given system. A second parameter obtained from SVD is the condition number, γ, which is the ratio between the maximum and minimum singular values:

$$\gamma = \sigma^*/\sigma_* \tag{1}$$

The condition number measures the sensibility to the system to uncertainties in process parameters and modeling errors. Also, difficulties to decouple the control loop interaction may occur for systems with high values of the condition number [27]. Thus, low values of γ are desired. Once the SVD has been performed, the minimum singular value and condition number are obtained for each case, and their values are compared to establish the best sequences in terms of open-loop properties.

3.2 Closed-Loop Analysis

The closed-loop analysis was based on PI controllers due to the widespread use of this type of controllers for industrial distillation systems. For tuning up the controller parameters, propor-

1) List of symbols at the end of the paper.

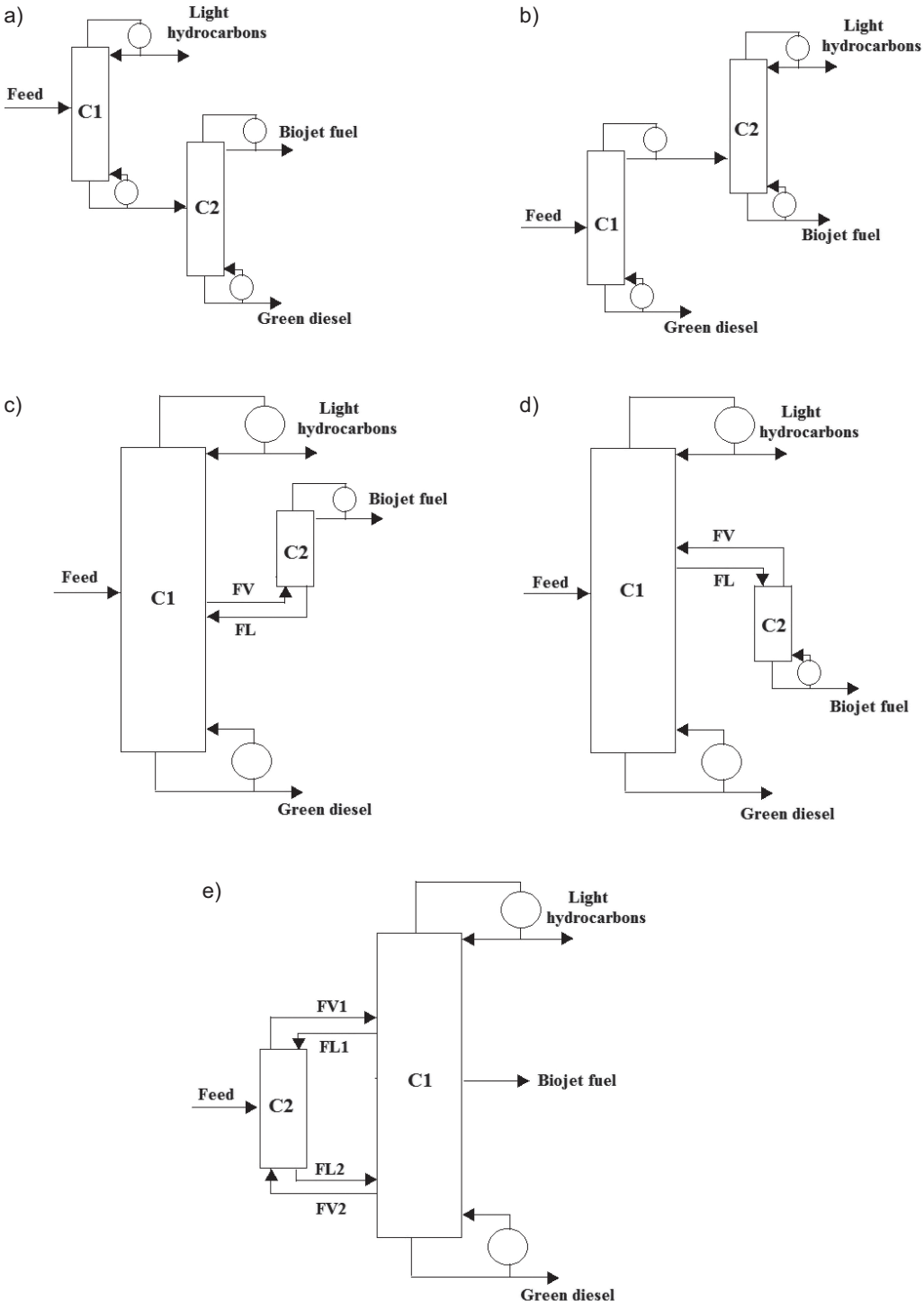

Figure 2. Sequences under study: (a) direct conventional sequence (CDS), (b) indirect conventional sequence (CIS), (c) thermally coupled direct sequence (TCDS), (d) thermally coupled indirect sequence (TCIS), (e) Petlyuk column.

tional gains (K_c) and the integral time constant (τ_i) were optimized for each scheme using the criterion of the IAE:

$$IAE = \int_0^\infty |\varepsilon(t)| \mathrm{d}t \tag{2}$$

where $\varepsilon(t)$ is the error in the time, which is given by:

$$\varepsilon(t) = y_d - y(t) \tag{3}$$

For each closed loop, the following methodology was performed: Set an initial value of the proportional gain and search

over a range of the integral time values until a local optimum value of IAE is found. The best configurations are those with the lowest IAE with its corresponding K_c and τ_i. Thus, these values are optimized for each sequence through a parametric analysis approach following the methodology reported in Fig. 3. Other tuning methods have been reported, such as the Biggest Log Modulus (BLT), the sequential loop closing (SLC) and the multi-loop modified Ziegler-Nichols method (MMZN) [28]. Nevertheless, the proposed approach takes advantage of the controller models already available on the dynamic simulator.

During the dynamic analysis, single set point changes for product composition were implemented on the C3 product stream and the *n*-C18 product stream; these were considered as the key components because they have the highest contents of the light hydrocarbon and green diesel cuts, respectively. A well-known structure was implemented, in order to select and control outputs to be manipulated variables for each control loop [29, 30]. This commonly applied structure is based on energy balance considerations, which is called an LV control structure. This structure considers the reflux flow rate L and the vapor boil-up rate V as control variables in the distillate and bottoms output compositions [31]. Other pairings between variables can be obtained through the relative gain array (RGA), the relative exergy array (REA), and other methodologies [32]. Although, in practice, it is more common to use temperature controllers, the use of composition control structures is useful for comparative studies, and they have been widely used in previous works to detect the thermally coupled distillation system with the best closed-loop dynamic responses for both set point tracking and load rejection [10, 15, 33].

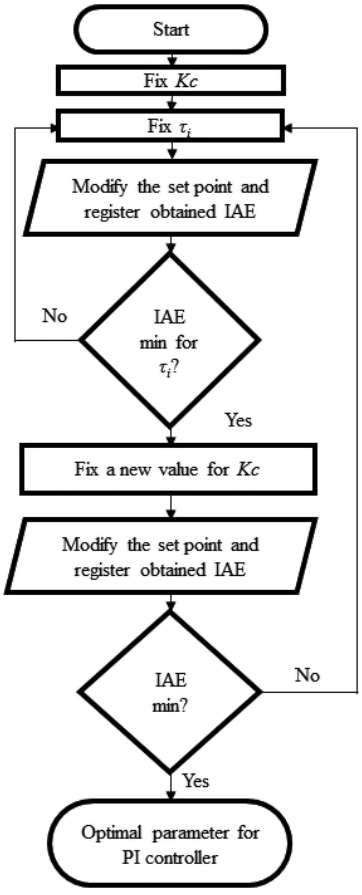

Figure 3. Methodology for the minimization of IAE.

4 Results

In this section, results for the control analysis will be presented and discussed. First, open-loop results are commented, followed by the analysis of the closed-loop results.

4.1 Results for Open-Loop Analysis

As mentioned before, to perform the SVD analysis, it is necessary to obtain dynamic responses when the system is perturbed. An example of the resulting responses for the conventional sequence CDS-S2 is shown in Fig. 4, corresponding to

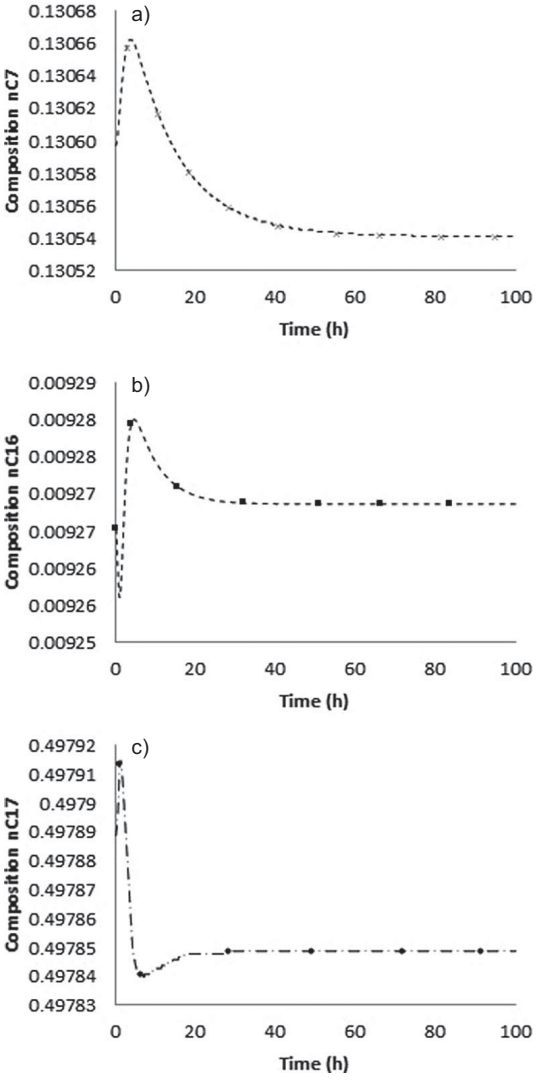

Figure 4. Open-loop responses for the sequence CDS-S2: (a) *n*-C7, (b) *n*-C16, (c) *n*-C17.

the response when a positive step change in the reflux ratio of the first column was implemented. As can be observed, all the obtained responses for the presented case are are of the competitive kind and show inverse responses. Once the responses for all the sequences are obtained, the transfer function matrices are constructed. Examples of transfer function matrices for a conventional sequence and a thermally coupled sequence are presented in Scheme 1. Those matrices correspond to the CDS-S2 case and the TCDS-S2 case when the composition of *n*-C7, *n*-C8, and *n*-C17 are the measured variables. For CDS-S2, R1 implies that the perturbation occurs at the reflux ratio of the first column, R2 is a perturbation of the reflux ratio of the second column, and Q2 implies a perturbation of the heat duty of the second column. Similarly, for TCDS-S2, R1 represents a perturbation of the reflux ratio on the main column, Q1 is a perturbation of the heat duty of the main column, and R2 implies that the perturbation occurs at the reflux ratio of the side rectifier. It can be seen that almost all the transfer functions are in competence. Nevertheless, first- and second-order responses were also observed for other sequences and cases.

Values for the minimum singular value for the distinct cases of the CDS are shown in Fig. S1 a in the Supporting Information, while in Fig. S1 b such values are presented for the TCDS when the contents of *n*-C7, *n*-C8, and *n*-C17 are the measured variables. In the case of the conventional sequence, it can be seen that the cases S1 and S2 show high values of $\sigma*$ for a wide range of frequencies. The case S5 shows high values for the minimum singular value only at very low frequencies. For the TCDS, the case S1 shows the highest values of $\sigma*$, followed by the cases S4 and S5. In Fig. S2, the values of the condition number for CDS and TCDS are presented. For the CDS, the case S1 shows low values of γ for high frequencies, while S2 and S5 show the best values at low frequencies. For the TCDS, the case S4 shows the lowest condition number values, while the case S1 shows low values for γ only at low frequencies. It can be seen that, for the conventional sequence, the cases with the lowest energy requirements show the best control properties. Nevertheless, for the thermally coupled system, the sequence with the lowest energy requirements shows good values for $\sigma*$, but only regular values of the condition number. The thermally coupled sequence with the best control properties is, thus, the case S4, located in the middle region of the Pareto front.

Fig. 5 shows the minimum singular value and the condition number for the best cases of each sequence under study. In terms of the minimum singular value, the TCIS shows good values for low frequencies, but it is the worst option at high frequencies. The DWC shows good values of $\sigma*$ for all the frequencies; nevertheless, it is important to recall that the DWC has very high energy requirements in comparison with the rest of the schemes. The other three systems (CDS, CIS and TCDS) show similar values of $\sigma*$ for all the frequencies. Nevertheless, if the condition number is analyzed, it can be seen that the CDS shows high condition number values for low frequencies, while CIS shows high values of γ for high frequencies. Both thermally coupled sequences (TCDS and TCIS) show good values of the condition number, but the direct thermally coupled sequence shows more stability on its γ profile for the whole range of frequencies. Thus, if only the open-loop control properties are analyzed, the best design in terms of controllability is the S4 of the thermally coupled direct distillation sequence, which does not have the lowest energy duty among the selected Pareto points for the TCDS, but the difference from the design S1 (the one with the lowest energy requirements) is only about 11 %.

4.2 Results for the Closed-Loop Analysis

In this section, results for the closed-loop analysis will be presented. The study was performed only for the cases S1, S3, and S5, because case S2 is expected to have a behavior similar to that of S1, S4 similar to S3, and so on. Only for the DWC, cases S2 and S4 are studied. Some representative results will be discussed. In Fig. 6, dynamic responses are shown for the CDS-S1 (a) and the TCDS-S1 (b), when the proportional gain is set as 10. It can be seen that the conventional system is stabilized at a shorter time than the thermally coupled sequence. Nevertheless, the thermally coupled column allows reaching

CDS-S2

$$\begin{array}{c} \\ \text{R1} \\ \text{R2} \\ \text{Q2} \end{array} \begin{array}{c} \text{C7} \\ \left[\begin{array}{c} \frac{0.026}{1+1.88742s}+\frac{-0.0484}{1+11.983s} \\ \frac{0.026}{1+1.8899s}+\frac{-0.0484}{1+11.984s} \\ \frac{0.0264}{1+1.9501s}+\frac{-0.0488}{1+11.9042s} \end{array}\right. \end{array} \begin{array}{c} \text{C16} \\ \begin{array}{c} \frac{-0.003688}{7.44s+1}+\frac{0.005012}{55.45s^2+1.89s+1} \\ \frac{-0.003692}{0.1036s+1}+\frac{0.005016}{0.0107s^2+0.7s+1} \\ \frac{-0.003688}{7.44s+1}+\frac{0.005012}{55.46s^2+1.89s+1} \end{array} \end{array} \begin{array}{c} \text{C17} \\ \left.\begin{array}{c} \frac{0.01039}{4.58s+1}+\frac{-0.0264}{21.02s^2+3.23s+1} \\ \frac{0.01039}{0.809s+1}+\frac{-0.0264}{0.655s^2+2.056s+1} \\ \frac{0.01039}{4.55s+1}+\frac{-0.0264}{20.72s^2+3.24s+1} \end{array}\right] \end{array}$$

TCDS-S2

$$\begin{array}{c} \\ \text{R1} \\ \text{Q1} \\ \text{R2} \end{array} \begin{array}{c} \text{C7} \\ \left[\begin{array}{c} 0 \\ 0 \\ 0 \end{array}\right. \end{array} \begin{array}{c} \text{C16} \\ \begin{array}{c} \frac{0.000212}{1+2.815s}+\frac{-0.000816}{1+26.61s} \\ \frac{0.000212}{1+2.817s}+\frac{-0.000812}{1+26.261s} \\ \frac{0.000212}{1+2.823s}+\frac{-0.000812}{1+26.267s} \end{array} \end{array} \begin{array}{c} \text{C17} \\ \left.\begin{array}{c} \frac{-0.0008}{1+5.6903s}+\frac{0.00039}{1+20.42s} \\ \frac{-0.0008}{1+5.6902s}+\frac{0.00039}{1+20.43s} \\ \frac{-0.0008}{1+5.687s}+\frac{0.00039}{1+20.44s} \end{array}\right] \end{array}$$

Scheme 1. Matrices of transfer functions for CDS-S2 and TCDS-S2.

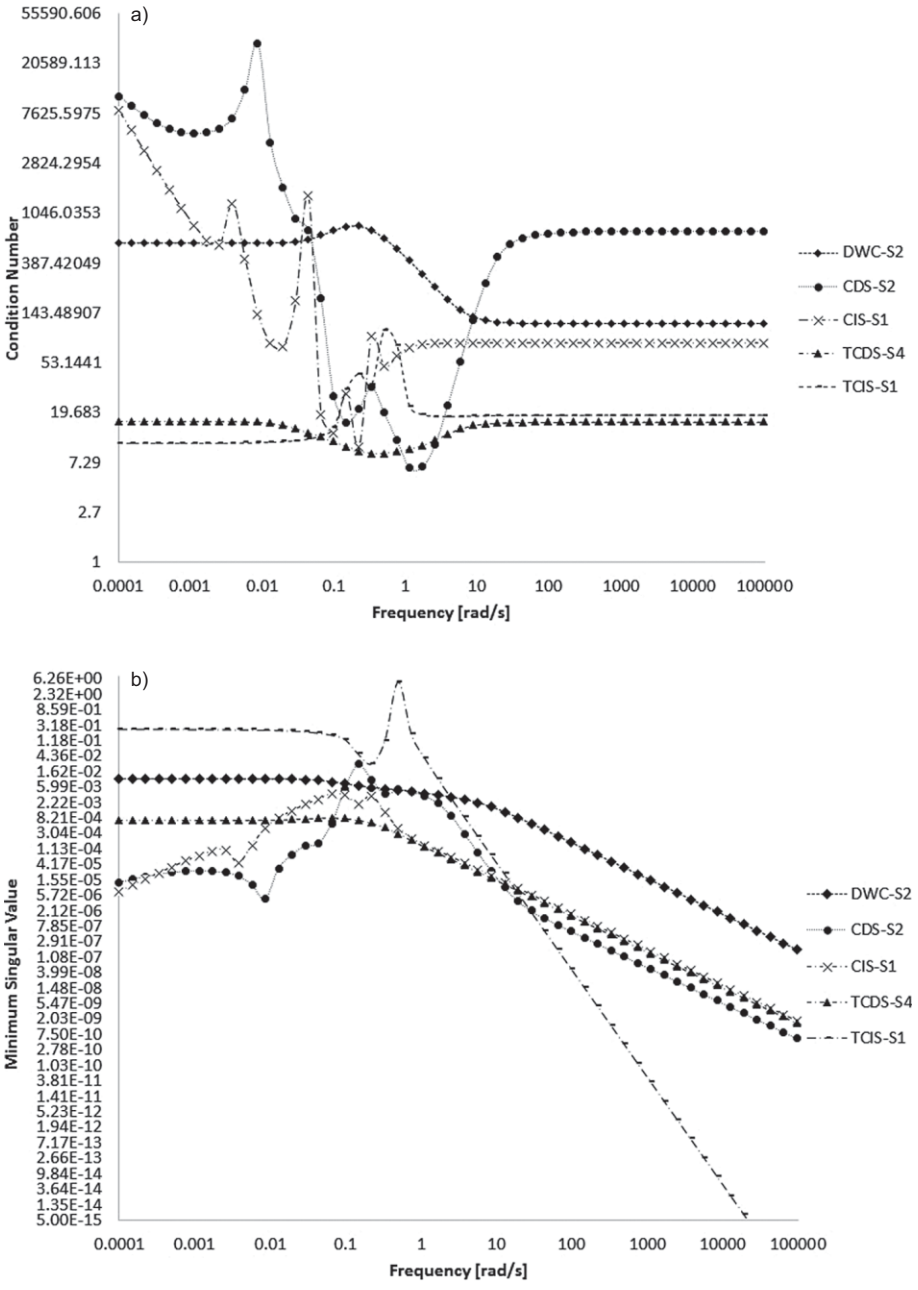

Figure 5. Dynamic properties for the best case of each sequence: (a) condition number, (b) minimum singular value.

the new set point with less oscillation at lower values of the integral time. In Fig. 7, the IAE for C3 is shown for different values of K_c and τ_i, for both CDS-S1 (a) and TCDS-S1 (b). It can be seen that, in the case of the conventional direct sequences, values of K_c higher than 90 allow low values of the IAE. Furthermore, the best values of IAE are obtained for low integral time values. In the case of the thermally coupled sequence, low values of IAE are obtained for proportional gains higher than 30, and the best values for this sequence are obtained for high values of τ_i. It can be observed that the maximum value of the integral time for the thermally coupled sequence (50 min) is among the lowest feasible values for the conventional sequence. In other words, for similar values of IAE, the thermally coupled sequence requires lower values for the integral time than the conventional sequence. In Tab. 2, a comparison between the best values of IAE for each sequence and component is presented. In the case of the CDS, it can be seen that the best values of IAE occur for the design with the highest energy requirements in the Pareto front for that kind of sequence (CDS-S5). For the CIS, the case with the lowest values of IAE for both components is, once more, that with the highest energy duty (CIS-S5). In the case of the TCDS, the cases S1 and S3 show relatively good IAE values when the composition of C3 is controlled, but the design S5 shows the best values when the content of *n*-C18 is analyzed. Nevertheless, that case (S5) could not be stabilized in the new set point for C3. If the

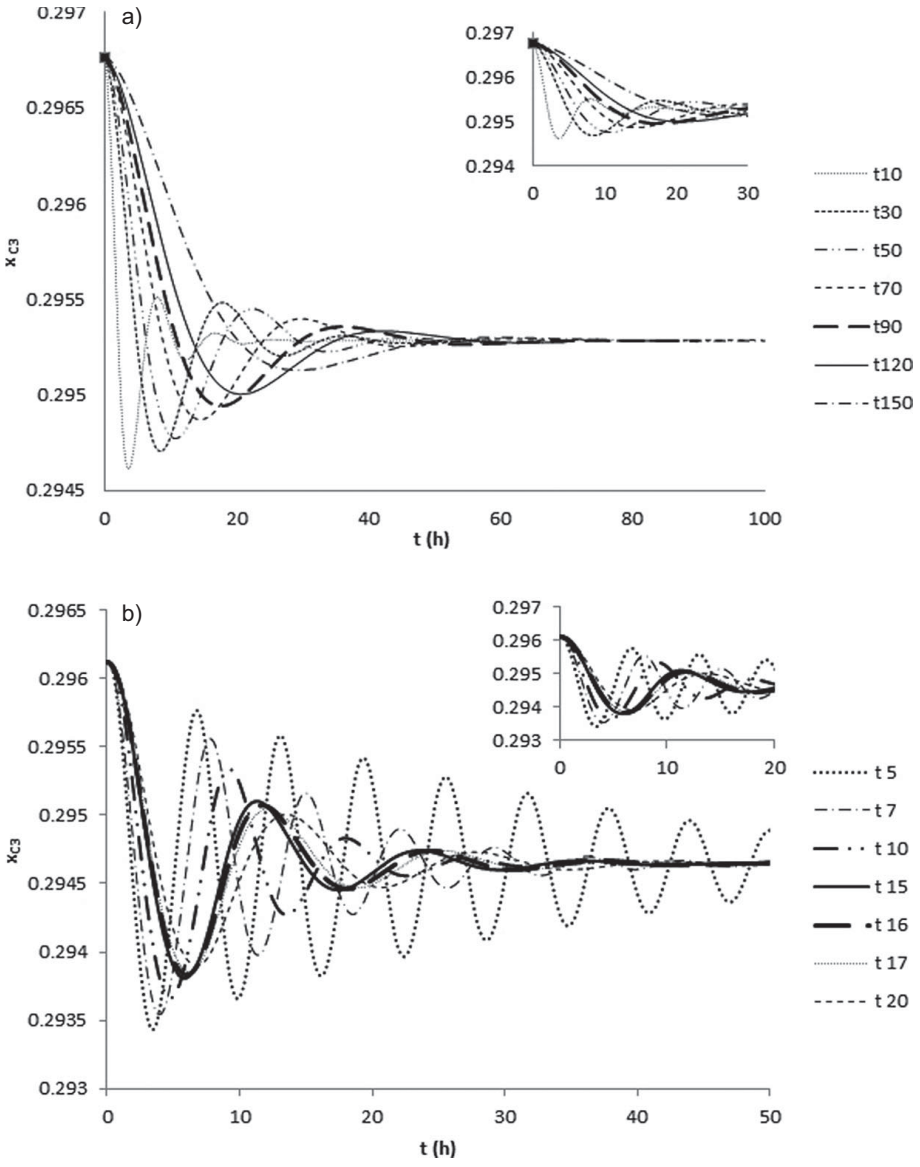

Figure 6. Dynamic responses for component C3 with $K_c = 10$: (a) CDS-S1, (b) TCDS-S1.

results for the TCIS are analyzed, the case with an intermediate heat duty (S3) shows the lowest values of IAE. Finally, there is no observable difference between the IAE values for both cases of DWC. If all the studied sequences are compared, it can be seen that the TCIS and the DWC show the lowest values for IAE. Nevertheless, the DWC has considerably high energy requirements when compared to the other sequences. The TCIS has values of heat duty comparable with those of the conventional sequences. The sequence with the lowest heat duties, i.e. the TCDS, has the highest values of IAE. Still, the values of that criterion can be acceptable when considering the savings in terms of energy requirements for the TCDS sequences.

5 Conclusions

A dynamic study of distillation sequences for the purification of bio-jet fuel and green diesel was presented. The analyzed sequences include conventional and thermally coupled trains, where the thermally coupled distillation sequence shows the lowest heat duty among all the sequences. Different cases, from the low- to the high-duty regions of the Pareto front, were selected and studied through open-loop and closed-loop methods. The open-loop results show different performances for the distillation sequences when low and high frequencies are taken into account, and the closed-loop results give detailed information on the dynamic performance of the systems. The sequences with the best closed-loop performances are the DWC and the TCIS, but they have high energy requirements. The TCDS has high values of the IAE criterion when compared with the other sequences; nevertheless, they can be acceptable values to achieve

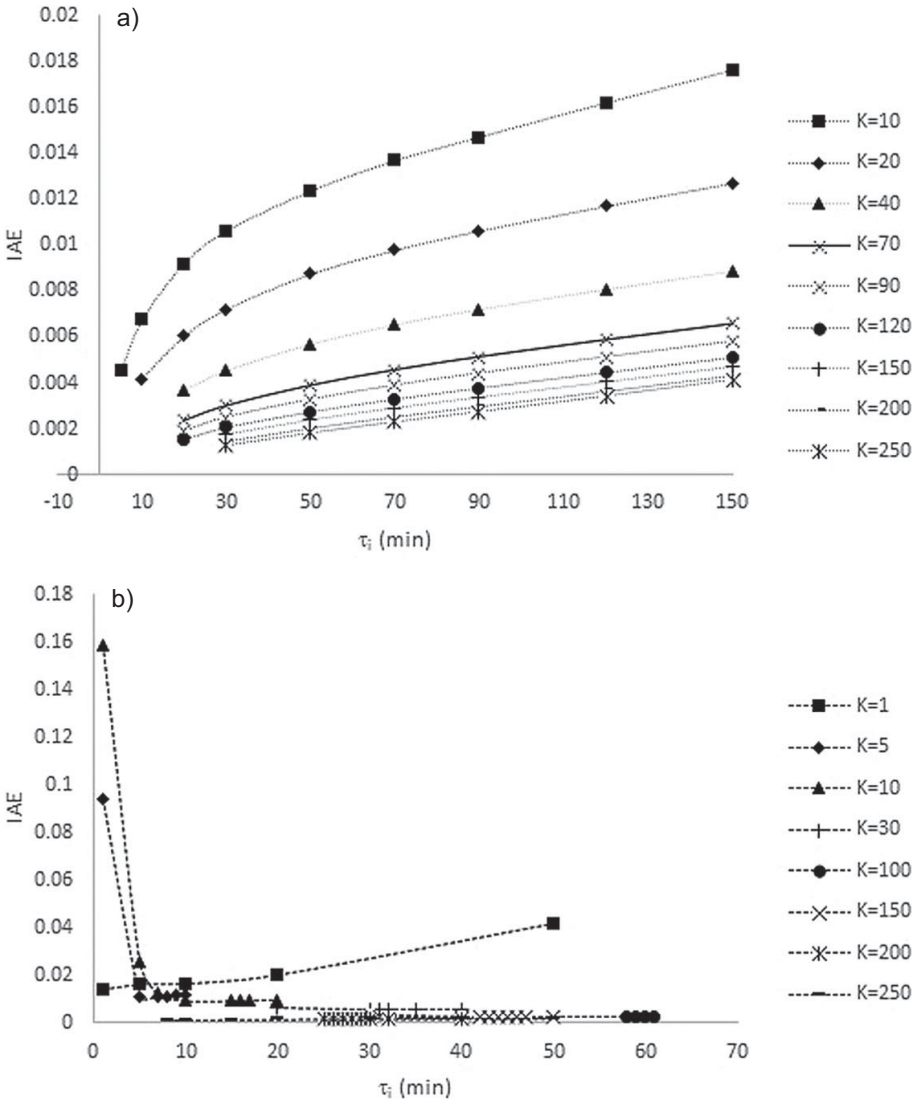

Figure 7. Variation of IAE for component C3 with the proportional gain and the integral time: (a) CDS-S1, (b) TCDS-S1.

Table 2. Comparison of the best values of IAE for each sequence.

Sequence/component	K_c [%/%]	τ_i [min]	IAE [–]
CDS-S1/C3	250	30	0.00126043
CDS-S1/*n*-C18	250	1	7.9596×10^{-5}
CDS-S3/C3	250	10	0.00044778
CDS-S3/*n*-C18	250	1	9.5624×10^{-5}
CDS-S5/C3	250	2	6.70041×10^{-5}
CDS-S5/*n*-C18	250	1	6.4967×10^{-5}
TCDS-S1/C3	250	8	0.00126691
TCDS-S1/*n*-C18	9	19	0.00346796
TCDS-S3/C3	250	23	0.00110955
TCDS-S3/*n*-C18	70	1	0.00101338
TCDS-S5/C3	–	–	–

Table 2. Continued.

Sequence/component	K_c [%/%]	τ_i [min]	IAE [–]
TCDS-S5/*n*-C18	250	1	4.7556×10^{-5}
DWC-S2/C3	250	1	2.4171×10^{-5}
DWC-S2/*n*-C18	250	1	4.0361×10^{-5}
DWC-S4/C3	250	1	2.4169×10^{-5}
DWC-S4/*n*-C18	250	1	4.0395×10^{-5}
CIS-S1/C3	13	1	0.00116035
CIS-S1/*n*-C18	250	1	5.0372×10^{-5}
CIS-S3/C3	27	1	0.00064566
CIS-S3/*n*-C18	250	1	5.0463×10^{-5}
CIS-S5/C3	250	1	0.00031387
CIS-S5/*n*-C18	250	1	3.5595×10^{-5}
TCIS-S1/C3	250	2	4.3502×10^{-5}
TCIS-S1/*n*-C18	250	1	6.4012×10^{-5}
TCIS-S3/C3	250	1	2.55906×10^{-5}
TCIS-S3/*n*-C18	250	1	5.3552×10^{-5}
TCIS-S5/C3	250	1	4.3925×10^{-5}
TCIS-S5/*n*-C18	250	1	6.2029×10^{-5}

low heat duties and, as a consequence, reduced environmental impact due to the process. Of course, to achieve such dynamic responses, proper tuning of the controller parameters is critical.

Acknowledgment

The authors acknowledge the financial support of CONACYT, through project 239765, Universidad de Guanajuato, México, and Universidad Autónoma de Querétaro, México.

The authors have declared no conflict of interest.

Symbols used

IAE	[–]	integral of the absolute error
K_c	[–]	proportional gain of the controller
t	[h]	time
$\mathbf{V}$	[–]	matrix of left singular vectors
$\mathbf{W^H}$	[–]	matrix of right singular vectors
y_d	[–]	set point
$y(t)$	[–]	value of the measured variable in a given time

Greek symbols

γ	[–]	condition number
$\varepsilon(t)$	[–]	error in the time
$\sigma*$	[–]	minimum singular value
σ^*	[–]	maximum singular value
Σ	[–]	matrix of singular values
τ_i	[min]	integral time constant of the controller

Abbreviations

CDS	direct conventional distillation sequence
CIS	indirect conventional distillation sequence
DWC	dividing-wall column
IAE	integral of the absolute error
PI	proportional-integral
PID	proportional-integral-derivative
SPK	synthetic paraffinic kerosene
SVD	singular value decomposition
TCDS	thermally coupled direct sequence
TCIS	thermally coupled indirect sequence

References

[1] Air Transport Action Group (ATAG), *Facts and figures of air transport*, www.atag.org/facts-and-figures.html, **2014** (Accessed on April 15, 2015).
[2] European Commission, *Reducing emissions from the aviation sector*, ec.europa.eu, **2014** (Accessed on June 28, 2015).
[3] ASTM Standard D7566, ASTM International, PA, www.astm.org, **2014**. DOI: 10.1520/D7566-14A
[4] J. A. Kocal, R. E. Marinangeli, T. L. Marker, M. J. McCall, *U.S. Patent 158637-A1*, **2009**.

[5] C. Gutiérrez-Antonio, F. I. Gómez-Castro, S. Hernández, A. Briones-Ramírez, *Chem. Eng. Process.* **2015**, *88*, 29–36. DOI: 10.1016/j.cep.2014.12.002
[6] S. Hernández, A. Jiménez, *Ind. Eng. Chem. Res.* **1999**, *38 (10)*, 3957–3963. DOI: 10.1021/ie990103u
[7] A. Jiménez, S. Hernández, F. A. Montoy, M. Zavala-García, *Ind. Eng. Chem. Res.* **2001**, *40 (17)*, 3757–3761. DOI: 10.1021/ie000047t
[8] F. I. Gómez-Castro, J. G. Segovia-Hernández, S. Hernández, C. Gutiérrez-Antonio, A. Briones-Ramírez, *Chem. Eng. Technol.* **2008**, *31 (9)*, 1246–1260. DOI: 10.1002/ceat.200800116
[9] F. I. Gómez-Castro, M. A. Rodríguez-Ángeles, J. G. Segovia-Hernández, S. Hernández, C. Gutiérrez-Antonio, A. Briones-Ramírez, A. R. Uribe-Ramírez, *Ind. Eng. Chem. Res.* **2013**, *52 (29)*, 9922–9929. DOI: 10.1021/ie401332p
[10] K. S. Hwang, B. C. Kim, Y. H. Kim, *Chem. Eng. Technol.* **2011**, *34 (2)*, 273–281. DOI: 10.1002/ceat.200900483
[11] J. G. Segovia-Hernández, S. Hernández, A. Jiménez, *Trans. IChemE* **2002**, *80 (7)*, 783–789. DOI: 10.1205/02638760 2320776858
[12] Y. Zhu, X. Liu, J. Qian, *Proceedings of the 5th World Congress on Intelligent Control and Automation*, Hangzhou **2004**, 3445–3449. DOI: 10.1109/WCICA.2004.1343184
[13] J. G. Segovia-Hernández, S. Hernández, A. Jiménez, R. Femat, *Chem. Biochem. Eng. Q.* **2005**, *19 (3)*, 243–253. DOI: 21744,35400013167185.0030
[14] J. G. Segovia-Hernández, E. A. Hernández-Vargas, J. A. Márquez-Muñoz, *Comput. Chem. Eng.* **2007**, *31 (7)*, 867–874. DOI: 10.1016/j.compchemeng.2006.08.004
[15] H. Ling, W. L. Luyben, *Ind. Eng. Chem. Res.* **2009**, *48 (13)*, 6034–6049. DOI: 10.1021/ie801373b
[16] C. Buc, C. Hiller, G. Fieg, *Chem. Eng. Technol.* **2011**, *34 (5)*, 663–672. DOI: 10.1002/ceat.201000487
[17] X. Liu, L. Cong, Y. Zhou, *Ind. Eng. Chem. Res.* **2013**, *52 (19)*, 6470–6479. DOI: 10.1021/ie400033h
[18] R. K. Dohare, K. Singh, R. Kumar, *Syst. Sci. Control Eng.* **2015**, *3 (1)*, 142–153. DOI: 10.1080/21642583.2014.996301
[19] S. Tututi-Ávila, A. Jiménez-Gutiérrez, *Ind. Eng. Chem. Res.* **2013**, *52 (22)*, 7492–7503. DOI: 10.1021/ie302836y
[20] N. Ramírez-Corona, D. Mascote-Pérez, A. Sánchez-Hijar, M. I. Fernández-Pastrana, A. Jiménez-Gutiérrez, *Chem. Eng. Res. Des.* **2015**, *93*, 120–135. DOI: 10.1016/j.cherd.2014.05.015
[21] C. S. Bildea, A. A. Kiss, *Chem. Eng. Res. Des.* **2011**, *89 (2)*, 187–196. DOI: 10.1016/j.cherd.2010.05.007
[22] R. Murrieta-Dueñas, R. Gutiérrez-Guerra, J. G. Segovia-Hernández, S. Hernández, *Chem. Eng. Res. Des.* **2011**, *89 (11)*, 2215–2227. DOI: 10.1016/j.cherd.2011.02.021
[23] R. M. Ignat, A. A. Kiss, *Chem. Eng. Res. Des.* **2013**, *91 (9)*, 1760–1767. DOI: 10.1016/j.cherd.2013.02.009
[24] J. K. Cheng, C. C. Chao, J. D. Ward, I. L. Chien, *J. Taiwan Inst. Chem. E* **2014**, *45 (1)*, 76–84. DOI: 10.1016/j.jtice.2013.04.005
[25] I. D. Gil, J. M. Gómez, G. Rodríguez, *Comput. Chem. Eng.* **2012**, *39*, 129–142. DOI: 10.1016/j.compchemeng.2012.01.006
[26] J. G. Segovia-Hernández, M. Vázquez-Ojeda, F. I. Gómez-Castro, C. Ramírez-Márquez, M. Errico, S. Tronci, B. G. Rong, *Chem. Eng. Process.* **2014**, *75*, 119–125. DOI: 10.1016/j.cep.2013.11.002
[27] O. Santolík, M. Parrot, F. Lefeuvre, *Radio Sci.* **2003**, *38 (1)*, 1010–1011. DOI: 10.1029/2000RS002523
[28] E. M. Ali, *Eng. Sci.* **2002**, *14 (2)*, 183–198.
[29] J. G. Segovia-Hernández, S. Hernández, R. Femat, A. Jiménez, *Ind. Eng. Chem. Res.* **2007**, *46 (2)*, 546–558. DOI: 10.1021/ie060438t
[30] J. G. Segovia-Hernández, S. Hernández, V. Rico-Ramírez, A. Jiménez, *Comput. Chem. Eng.* **2004**, *28 (5)*, 811–819. DOI: 10.1016/j.compchemeng.2004.02.019
[31] K. E. Häggblom, K. V. Waller, *Practical Distillation Control*, 1st ed., Springer, New York **1993**.
[32] F. Osuolale, J. Zhang, *Chem. Eng. Technol.* **2015**, *38 (5)*, 907–916. DOI: 10.1002/ceat.201400707
[33] D. Dwivedi, I. J. Halvorsen, S. Skogestad, *Chem. Eng. Process.* **2012**, *67*, 49–59. DOI: 10.1016/j.cep.2012.07.013

